A lattice hydrodynamical model considering turning capability*

Tian Huan-Huan(田欢欢)[a)b)] and Xue Yu(薛 郁)[a)c)†]

[a)] *Shanghai Institute of Applied Mathematics and Mechanics, Shanghai University, Shanghai* 200072, *China*

[b)] *College of Physics Science and Engineering, Yulin Normal University, Yulin* 537000, *China*

[c)] *Institute of Physics Science and Engineering, Guangxi University, Nanning* 530004, *China*

(Received 20 November 2011; revised manuscript received 13 February 2012)

A new two-dimensional lattice hydrodynamic model considering the turning capability of cars is proposed. Based on this model, the stability condition for this new model is obtained by using linear stability analysis. Near the critical point, the modified KdV equation is deduced by using the nonlinear theory. The results of numerical simulation indicate that the critical point a_c increases with the increase of the fraction p of northbound cars which continue to move along the positive y direction for $c = 0.3$, but decreases with the increase of p for $c = 0.7$. The results also indicate that the cars moving along only one direction (eastbound or northbound) are most stable.

Keywords: modified KdV equation, traffic flow, lattice hydrodynamic model

PACS: 05.50.+q, 02.60.Cb, 84.40.Xb **DOI:** 10.1088/1674-1056/21/7/070505

1. Introduction

Traffic problems, especially traffic jams, are serious problems in modern society. To understand the dynamics of traffic flow and to investigate the properties of traffic jams, many traffic models[1−3] have been proposed by many scholars.

Previous studies indicate that traffic jams occur and propagate like density waves. Kerner and Konhäuser[4] discovered the single-pulse density wave based on a hydrodynamic model. The single-pulse density wave was proved to be a soliton by Kurtze and Hong.[5] The modified KdV (mKdv) equation, which is used to describe the kink density wave, was derived by Komatsu and Sasa[6] from the optimal velocity model. Muramatsu and Nagatani[7] further proved that the solitonary density wave appears only near the neutral stability line. Nagatani[8,9] proposed a lattice hydrodynamic model, and obtained the mKdV equation from that model in terms of the nonlinear theory. He also generalized the one-dimensional lattice hydrodynamic model to two dimensions,[10] two-lane traffic flow,[11] and a high-dimensional model.[12] From then on, many extended lattice hydrodynamic models[13−22] have been proposed to investigate the vehicular traffic. Tian,[23] Xue,[24] Wen,[25] and their coauthors extended the two-dimensional lattice hydrodynamics model to study pedestrian flow.

As we know, in realistic traffic, a driver or a walker is likely to change his or her direction to another stochastically independent of other vehicles or other walkers. A driver's or a walker's path from origination to destination is not always a straight line. The driver or walker is likely to save time by turning and taking shortcuts. Cuesta *et al.*[26] and Nagatani[27,28] have taken the turning capability of cars into account to study traffic in the Biham-Middleton-Levine model.

In this paper, a new two-dimensional lattice hydrodynamic model considering the turning capability of cars is proposed in Section 2. The linear stability analysis is carried out in Section 3 and the nonlinear analysis is conducted in Section 4. In Section 5, computer simulation is performed to explore the characteristics of the two-dimensional traffic flow. The last section provides a conclusion.

2. Model

According to the idea thought of by Cuesta *et al.*[26] and Nagatani,[27,28] and based on the two-dimensional lattice hydrodynamic model proposed by

*Project supported by the National Natural Science Foundation of China (Grant Nos. 10865001, 11047003, 11172164, and 11162019) and the Youth Foundation of the Yulin Normal University of China (Grant No. 2011YJQN01).

†Corresponding author. E-mail: yuxuegxu@gxu.edu.cn

© 2012 Chinese Physical Society and IOP Publishing Ltd

Nagatani,[10] we construct a new model in which the role of turning is considered. The model is described by means of the following differential–difference equations:

$$\partial_t \rho^x_{j,m} + \rho_{x0}[F_{j,m} - F_{j-1,m}] = 0, \quad (1)$$

$$\partial_t \rho^y_{j,m} + \rho_{y0}[G_{j,m} - G_{j,m-1}] = 0, \quad (2)$$

$$\begin{aligned}\partial_t F_{j,m} =\ & a[q\rho_{x0}V(\rho_{j+1,m}) \\ & + (1-q)\rho_{y0}V(\rho_{j,m+1})] - aF_{j,m}, \quad (3)\\ \partial_t G_{j,m} =\ & a[p\rho_{y0}V(\rho_{j,m+1}) \\ & + (1-p)\rho_{x0}V(\rho_{j+1,m})] - aG_{j,m}, \quad (4)\end{aligned}$$

where $\partial_t = \partial/\partial t$; $\rho^x_{j,m}$ and $\rho^y_{j,m}$ are the local density of eastbound cars (moving along the positive x direction) and northbound cars (moving along the positive y direction) on site (j,m) at time t, respectively; $1/\rho_{x0}$ and $1/\rho_{y0}$ denote the average headway of eastbound cars and northbound cars, respectively; $F_{j,m}$ and $G_{j,m}$ are the local flux of eastbound cars and northbound cars on site (j,m) at time t; q denotes the fraction of the eastbound cars which continue to move along the positive x direction; p denotes the fraction of the northbound cars which continue to move along the positive y direction; $a(=1/\tau)$ is the sensitivity of a driver, with τ being the delay time.

Equations (3) and (4) are the evolution equations of the local flux of eastbound and northbound cars, respectively. The local flux $F_{j,m}(t)$ of eastbound cars at time t, is adjusted by the optimal current $q\rho_{x0}V(\rho_{j+1},m)$ with a delay time τ at site $(j+1,m)$ and $(1-q)\rho_{y0}V(\rho_{j,m+1})$ at site $(j,m+1)$; the local flux $G_{j,m}(t)$ of northbound cars at site (j,m) at time t, is adjusted by the optimal current $p\rho_{yo}V(\rho_{j,m+1})$ with delay time τ at site $(j,m+1)$ and $(1-p)\rho_{xo}V(\rho_{j+1,m})$ at site $(j+1,m)$.

The optimal velocity function $V(\rho(j,m))$ is given as follows:[10]

$$V(\rho(j,m)) = \tanh\left(\frac{2}{\rho_0} - \frac{\rho(j,m)}{\rho_0^2} - \frac{1}{\rho_c}\right) + \tanh\left(\frac{1}{\rho_c}\right), \quad (5)$$

where ρ_c is the critical density, and ρ_0 is the total average density. By eliminating F and G in Eqs. (1) and (2), we obtain the following density equations:

$$\begin{aligned}\partial_t^2 \rho^x_{j,m} +\ & a\partial_t \rho^x_{j,m} + qa\rho^2_{x0}[V(\rho_{j+1,m}) - V(\rho_{j,m})] \\ & + (1-q)a\rho_{x0}\rho_{y0}[V(\rho_{j,m+1}) - V(\rho_{j,m})] \\ & = 0, \quad (6)\\ \partial_t^2 \rho^y_{j,m} +\ & a\partial_t \rho^y_{j,m} + pa\rho^2_{y0}[V(\rho_{j,m+1}) - V(\rho_{j,m})] \\ & + (1-p)a\rho_{x0}\rho_{y0}[V(\rho_{j+1,m}) - V(\rho_{j,m})] \\ & = 0. \quad (7)\end{aligned}$$

Let $\rho_{x0} = c\rho_0$ and $\rho_{y0} = (1-c)\rho_0$, where c is the fraction of eastbound cars at time $t = 0$. Then, on site (j,m) at time t, the expression of the local total density is: $\rho_{j,m} = \rho^x_{j,m} + \rho^y_{j,m}$. Consequently, the local total density equation on site (i,j) reads

$$\begin{aligned}\partial_t^2 \rho_{j,m} +\ & a\partial_t \rho_{j,m} + qac^2\rho_0^2[V(\rho_{j+1,m}) - V(\rho_{j,m})] \\ & + pa(1-c)^2\rho_0^2[V(\rho_{j,m+1}) - V(\rho_{j,m})] \\ & + ac(1-c)(1-q)\rho_0^2[V(\rho_{j,m+1}) - V(\rho_{j,m})] \\ & + ac(1-c)(1-p)\rho_0^2[V(\rho_{j+1,m}) - V(\rho_{j,m})] \\ & = 0. \quad (8)\end{aligned}$$

When $p = 0$ and $q = 0$, Eq. (8) is the density equation of the two-dimensional traffic flow.

3. Linear stability analysis

Now we carry out the linear stability analysis on Eq. (8). Suppose $\rho_{j,m} = \rho_0 + y_{j,m}$, where $y_{j,m}$ is a small deviation from the steady-state solution. Then, the linear equation is obtained from Eq. (8) as

$$\begin{aligned}\partial_t^2 y_{j,m} +\ & a\partial_t y_{j,m} + qac^2\rho_0^2 V'[y_{j+1,m} - y_{j,m}] \\ & + pa(1-c)^2\rho_0^2 V'[y_{j,m+1} - y_{j,m}] \\ & + ac(1-c)(1-q)\rho_0^2 V'[y_{j,m+1} - y_{j-1,m+1}] \\ & + ac(1-c)(1-p)\rho_0^2\rho_{y0} V'[y_{j+1,m} - y_{j+1,m-1}] \\ & = 0, \quad (9)\end{aligned}$$

where $V'(\rho_0) = [\mathrm{d}V/\mathrm{d}\rho]|_{\rho=\rho_0}$.

By using the Fourier-mode expansion $y_{j,m}(t) = \beta \exp[\mathrm{i}k(j+m) + zt]$, the above equation becomes

$$\begin{aligned}z^2 +\ & az + qac^2\rho_0^2 V'(\mathrm{e}^{\mathrm{i}k} - 1) \\ & + pa(1-c)^2\rho_0^2 V'(\mathrm{e}^{\mathrm{i}k} - 1) \\ & + ac(1-c)(1-q)\rho_0^2 V'(\mathrm{e}^{\mathrm{i}k} - 1) \\ & + ac(1-c)(1-p)\rho_0^2 V'(\mathrm{e}^{\mathrm{i}k} - 1) = 0. \quad (10)\end{aligned}$$

Substituting $z = z_1(\mathrm{i}k) + z_2(\mathrm{i}k)^2 + \cdots$ into Eq. (10), the first- and second-order terms of $\mathrm{i}k$ become

$$z_1 = -V'[qc^2 + p(1-c)^2 + c(1-c)(2-p-q)]\rho_0^2, \quad (11)$$

$$z_2 = -\frac{z_1^2}{a} - \frac{V'[qc^2 + p(1-c)^2 + c(1-c)(2-p-q)]\rho_0^2}{2}. \tag{12}$$

When $z_2 < 0$, the uniformly steady-state flow becomes unstable for long-wavelengths. The uniform flow is stable if $z_2 > 0$. Thus the neutral stable condition is given by

$$a = -2V'[qc^2 + p(1-c)^2 + c(1-c)(2-p-q)]\rho_0^2. \tag{13}$$

For small disturbances with long wavelengths, the uniform traffic is unstable if

$$a < -2V'[qc^2 + p(1-c)^2 + c(1-c)(2-p-q)]\rho_0^2. \tag{14}$$

Figure 1 shows the parameter space (ρ, a) for $c = 0.3$ and 0.7 with $q = 0.9$. The solid lines represent the neutral stability lines and the dashed lines correspond to the coexisting lines. The apex of each curve at $\rho = \rho_c$ and $a = a_c$ is a critical point. If $a > a_c$, the uniform flow is always stable irrespective of density. From Eq. (13), we find that when $c = 0.5$, the sensitivity $a = -\rho_0^2 V'$.

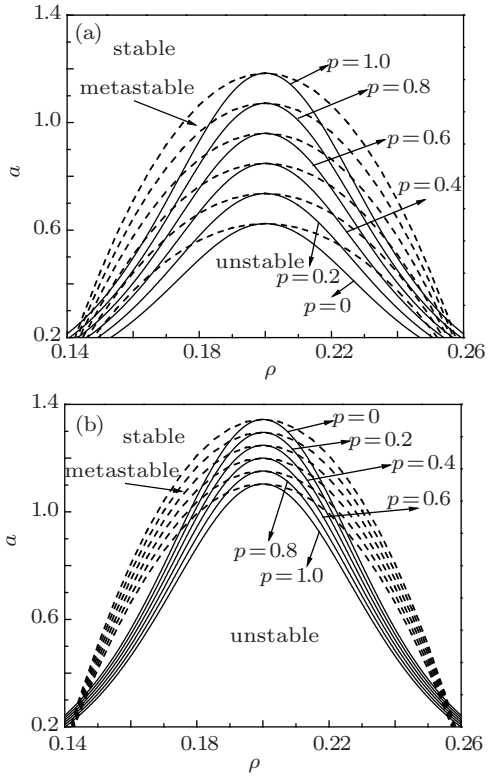


Fig. 1. Phase diagrams in the (ρ, a) plane for (a) $c = 0.3$ and (b) $c = 0.7$, respectively, with $q = 0.9$. The solid lines and dashed lines correspond to the neutral stability curves and the coexisting curves.

As shown in Fig. 1, the unstable region expands more and more with increasing rate p when $c = 0.3$, but shrinks more and more with increasing p when $c = 0.7$. In Fig. 1(a), $c = 0.3$ indicates that the number of the eastbound cars is less than that of the northbound cars, initially. If the northbound cars change their drive directions and move eastwards ($p = 0.0$), the stability of traffic flow can be enhanced. When the number of eastbound cars is larger than that of northbound ones at the beginning, keeping the northbound cars move northwards ($p = 1$) can help enhance the stability, as shown in Fig. 1(b). That is to say, if the cars on the high-density road change their drive direction and move along the low-density road, the stability of traffic flow can be enhanced.

4. Nonlinear analysis

The traffic behaviors of long-wavelength modes are investigated by virtue of the long-wave expansion near the critical point (ρ_c, τ_c). We define a slow variable X (T) in place of space variables j and m (time variable t) as follows:[10]

$$X = \varepsilon(j + m + bt), \quad T = \varepsilon^3 t, \tag{15}$$

where $0 < \varepsilon < 1$, and b is a constant determined later. We define the density as

$$\rho_{j,m}(t) = \rho_c + \varepsilon^3 R(X, T). \tag{16}$$

By expanding Eq. (8) to the fifth order of ε by using Eqs. (15) and (16), one obtain the following nonlinear partial differential equations:

$$\begin{aligned} a\varepsilon^2(b + f\rho_c^2 V')\partial_X R + \varepsilon^3(b^2 + a\frac{f\rho_c^2 V'}{2})\partial_X^2 R \\ + a\varepsilon^4(\partial_T R + \frac{f\rho_c^2 V'}{6}\partial_X^3 R + \frac{f\rho_c^2 V'''}{6}\partial_X R^3) \\ + \varepsilon^5(2b\partial_T\partial_X R \\ + a\frac{f\rho_c^2 V'}{24}\partial_X^4 R + a\frac{f\rho_c^2 V'''}{6}\partial_X^2 R^3 = 0, \end{aligned} \tag{17}$$

where

$$V' = [\mathrm{d}V(\rho)/\mathrm{d}\rho]|_{\rho=\rho_c}, \quad V''' = [\mathrm{d}^3 V(\rho)/\mathrm{d}\rho^3]|_{\rho=\rho_c},$$

and $f = qc^2 + p(1-c)^2 + c(1-c)(2-p-q)$. By defining $b = -f\rho_c^2 V'$, the second-order term of ε is eliminated

from the above equation. Near the critical point a_c, we have

$$\frac{a}{a_c} = 1 - \varepsilon^2. \tag{18}$$

By inserting Eq. (18) into the third-order terms in Eq. (17), we obtain

$$b^2 + a\frac{f\rho_c^2 V'}{2} = \frac{a_c^2}{4}\varepsilon^2, \tag{19}$$

By inserting Eq. (18) into Eq. (17), we obtain

$$\begin{aligned}\partial_T R = & -\frac{f\rho_c^2 V'}{6}\partial_X^3 R - \frac{f\rho_c^2 V'''}{6}\partial_X R^3 \\ & + \varepsilon\left(\frac{a_c}{4}\partial_X^2 R - \frac{f\rho_c^2 V'}{8}\partial_X^4 R\right. \\ & \left. - \frac{f\rho_c^2 V'''}{12}\partial_X^2 R^3\right) = 0. \end{aligned} \tag{20}$$

Using the following transformations:

$$\begin{aligned} T' &= \frac{-f\rho_c^2 V'}{6}T, \\ R(X,T') &= \sqrt{\frac{-f\rho_c^2 V'}{f\rho_c^2 V'''}}R'(X,T'), \end{aligned} \tag{21}$$

we obtain the regularized equation as follows:

$$\begin{aligned}\partial_{T'} R' = & \partial_X^3 R' - \partial_X R'^3 \\ & - \varepsilon\left[3\partial_X^2 R' + \frac{3}{4}\partial_X^4 R' - \frac{1}{2}\partial_X^2 R'^3\right] = 0. \end{aligned} \tag{22}$$

It is exactly the mKdV equation if we ignore the $O(\varepsilon)$ term in the above equation. The kink–antikink solution of the mKdV equation is given by

$$R'_0(X,T') = \sqrt{p}\tanh\sqrt{\frac{p}{2}}(X - pT'), \tag{23}$$

where p is the propagation velocity. We take into account the $O(\varepsilon)$ correction by assuming that $R'(X,T') = R'_0(X,T') + \varepsilon R'_1(X,T')$. In order to determine p for the kink solution, the solvability condition is necessary to be satisfied

$$(R'_0, M[R'_0]) = \int_{-\infty}^{+\infty} \mathrm{d}X R'_0 M[R'_0] = 0, \tag{24}$$

where $M[R'_0] = 3\partial_X^2 R' + 3\partial_X^4 R'/4 - \partial_X^2 R'^3/2$. Performing the integration, we obtain the selected velocity ($p = 5$) and the solution of the mKdV equation

$$R(X,T) = \sqrt{\frac{-5f\rho_c^2 V'}{f\rho_c^2 V'''}}\tanh\frac{5}{2}\left(X + \frac{5f\rho_c^2 V'}{6}T\right). \tag{25}$$

Replacing variables X and T with original variables j, m, and t, we obtain the following solution:

$$\begin{aligned}\rho_{j,m}(t) = & \rho_c \pm \sqrt{\frac{-5(2f\rho_c^2 V' + a)}{2f\rho_c^2 V'''}} \\ & \times \tanh\sqrt{\frac{5(2f\rho_c^2 V' + a)}{4f\rho_c^2 V'''}} \\ & \times \left(j + m + \frac{5a - 2f\rho_c^2 V'}{12}t\right). \end{aligned} \tag{26}$$

5. Simulation

Computer simulations have been carried out for the two-dimensional lattice hydrodynamic model considering the turning capability by Eq. (8). The fourth-order Runge–Kutta method and the periodic boundary are applied. The initial conditions are chosen as follows:

$$\begin{aligned}\rho_{j,m} = & \begin{cases} 0.1, & j = L/2, m = L/2, \\ 0.3, & j = L/2 - 1, m = L/2 - 1, \\ 0.2, & \text{otherwise}, \end{cases} \\ \partial_t \rho_{j,m} = & -qc^2\rho_0^2[V(\rho_{j+1,m}) - V(\rho_{j,m})] \\ & - p(1-c)^2\rho_0^2[V(\rho_{j,m+1}) - V(\rho_{j,m})] \\ & - c(1-c)(1-q)\rho_0^2[V(\rho_{j,m+1}) - V(\rho_{j,m})] \\ & - c(1-c)(1-p)\rho_0^2[V(\rho_{j+1,m}) \\ & - V(\rho_{j,m})], \end{aligned} \tag{27}$$

where the system size $L = 140$, $\rho_0 = \rho_c = 0.2$, and the time step is 0.12.

The phase diagram of (ρ, a)-space is given in Fig. 1. Obviously, the coexisting line (dashed line) and the neutral stability line (solid line) divide the traffic flow into three regions. The traffic flow at the region above each neutral stability line is stable, which means that the jam will not appear. However, the traffic flow at the region below each neutral stability line is unstable and the jam emerges. The region between the neutral stability line and the coexisting line is meta-stable. The coexisting lines are obtained from the solution of the mKdV equation (Eq. (27)).

Figure 2 is the evolution of traffic patterns for $q = 0.6$ and 0.8. The traffic jam is indicated by gray color which means that the density is higher than $\rho_0 = 0.2$ in this region. Jams occur within a small region at the beginning, and then spread to the whole system.

Figure 3 shows the traffic patterns on the single-horizontal road at $y = 50$, and on the single-vertical road at $x = 50$. The gray color indicates the traffic density is higher than $\rho_0 = 0.2$. The time evolution patterns for $q = 0.6$ are shown in Figs. 3(a) and 3(c), and the patterns for $q = 0.8$ are shown in Figs. 3(b) and 3(d). The gray jammed regions propagate backward.

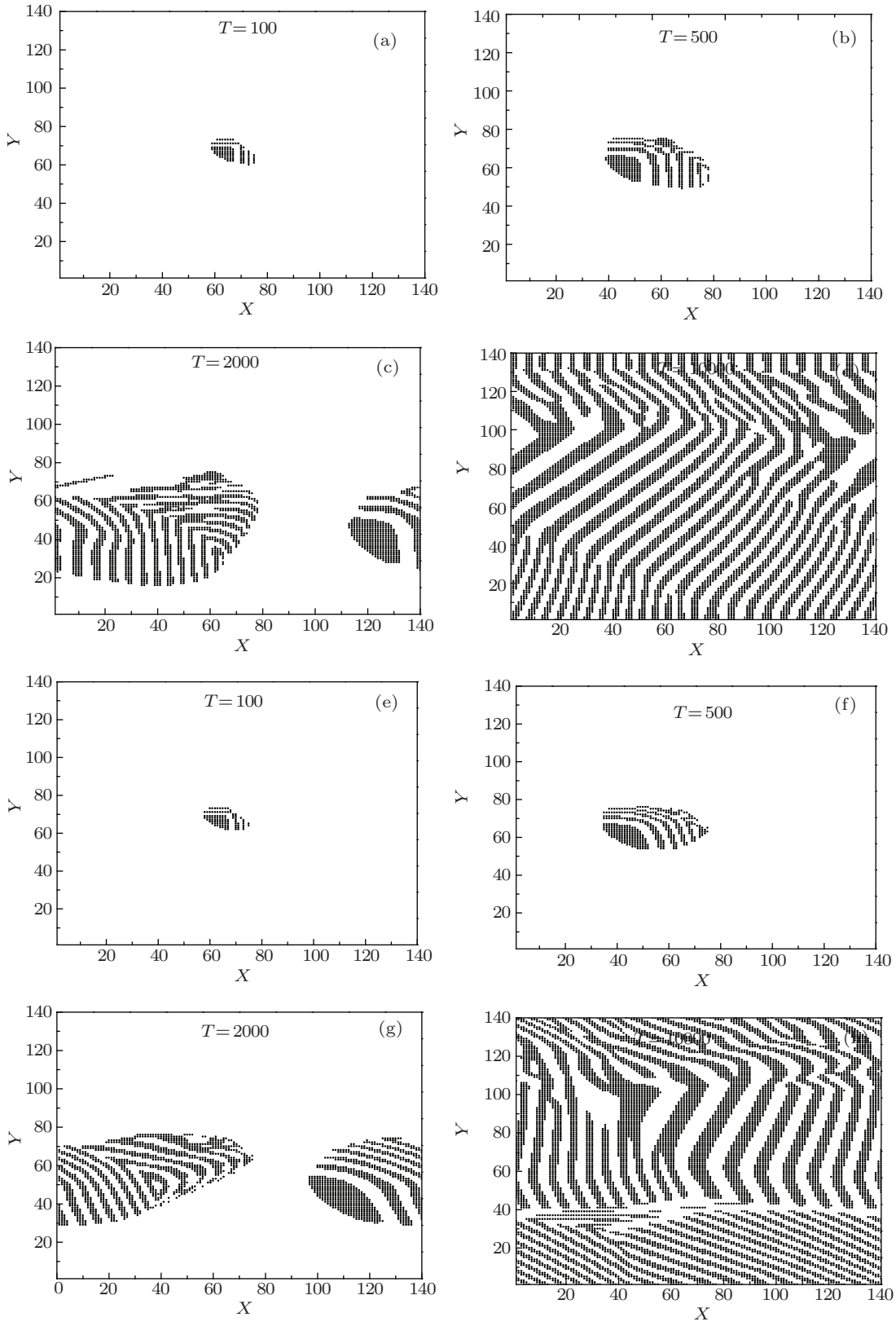


Fig. 2. Traffic patterns for different time-step numbers. (a), (e) $T = 100$; (b), (f) $T = 500$; (c), (g) $T = 2000$; (d), (h) $T = 10000$. $q = 0.6$ for (a), (b), (c), and (d); $q = 0.8$ for (e), (f), (g), and (h). $c = 0.7$, $p = 0.9$. The gray area indicates that the density is higher than $\rho_0 = 0.2$.

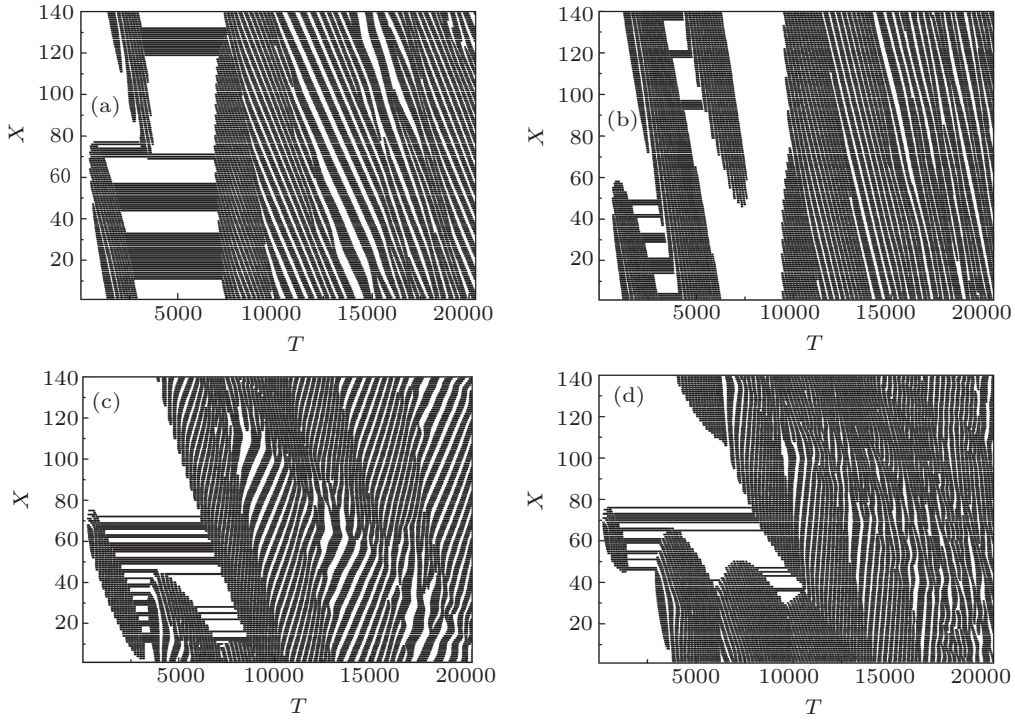


Fig. 3. Traffic patterns on the horizontal road at $y = 50$, and on the vertical road at $x = 50$. The gray area indicates that the traffic density is higher than $\rho_0 = 0.2$. (a), (c) $q = 0.6$; (b), (d) $q = 0.8$.

Figure 4 shows the time evolutions of the density after 20000 time steps under the different traffic turning probability with the sensitivity $a = 0.8$ for $c = 0.7$. Figures 4(a) and 4(c) show the time evolution of the density for $q = 0.6$, where $y = 50$ for Fig. 4(a) and $x = 50$ for Fig. 4(c). Figures 4(b) and 4(d) are the time evolution of the density for $q = 0.8$, $y = 50$, and $x = 50$, respectively. The density evolution is very similar to the solution of the mKdV equation.

Figure 5 shows the density profile obtained at time step $T = 15000$ with the sensitivity $a = 0.8$ for $c = 0.7$, $q = 0.6$ and 0.8, respectively. Figures 5(a) and 5(c) are density profiles for $q = 0.6$, $y = 50$, and $x = 50$, respectively. Figures 5(b) and 5(d) are density profiles for $q = 0.8$, $y = 50$, and $x = 50$, respectively.

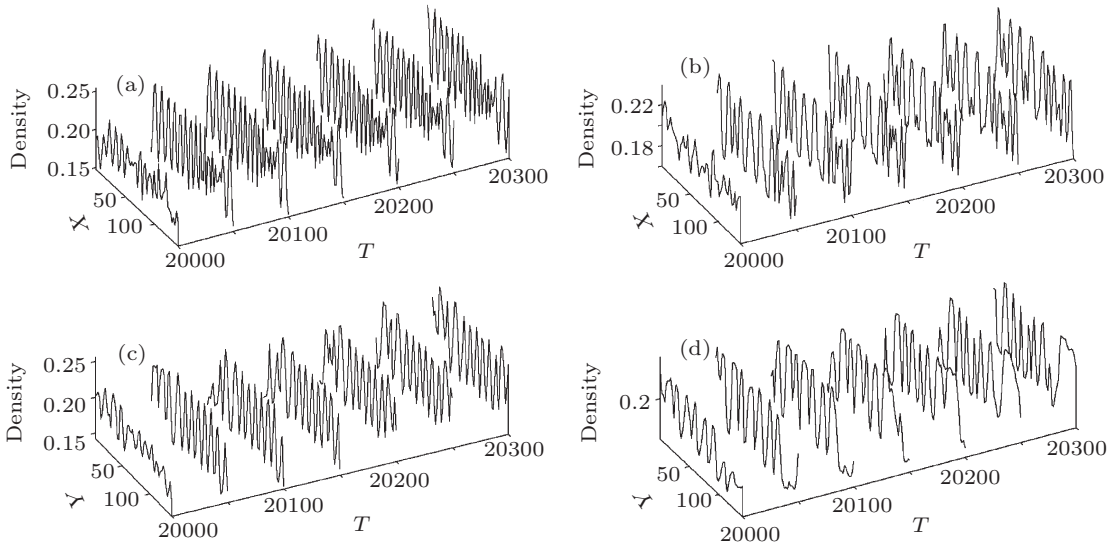


Fig. 4. Profiles of density after 20000 time steps for $a = 0.8$. (a) $q = 0.6$, $Y = 50$; (b) $q = 0.8$, $Y = 50$; (c) $q = 0.6$, $X = 50$; (d) $q = 0.8$, $X = 50$.

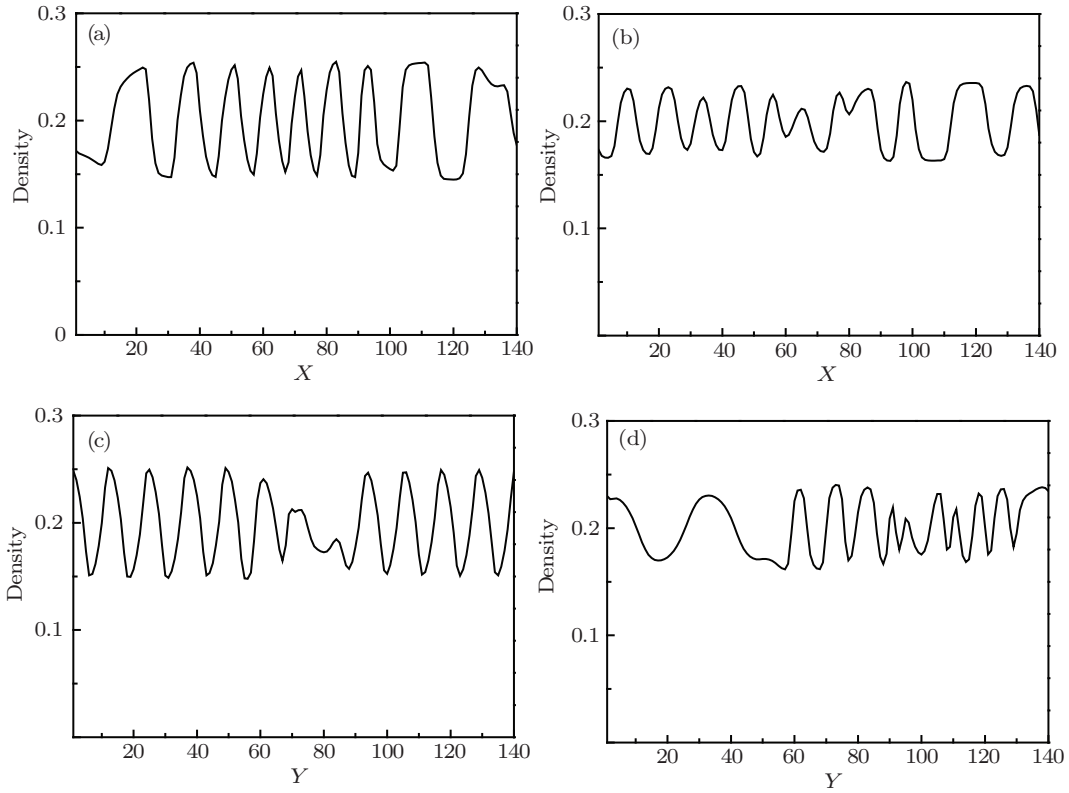


Fig. 5. Density profiles at $T = 15000$ for $c = 0.7$, $p = 0.9$, and $a = 0.8$. (a) $q = 0.6$, $Y = 50$; (b) $q = 0.8$, $Y = 50$; (c) $q = 0.6$, $X = 50$; (d) $q = 0.8$, $X = 50$.

Figure 6 shows plots of the critical sensitivity a_c against the parameters q and p. From Fig. 6, the critical sensitivity a_c is minimum when $q = 1.0$, $p = 0.0$ for $c = 0.3$, but $q = 0.0$, $p = 1.0$ for $c = 0.7$. That is to say, the cars moving along only one direction (east or north) are most stable.

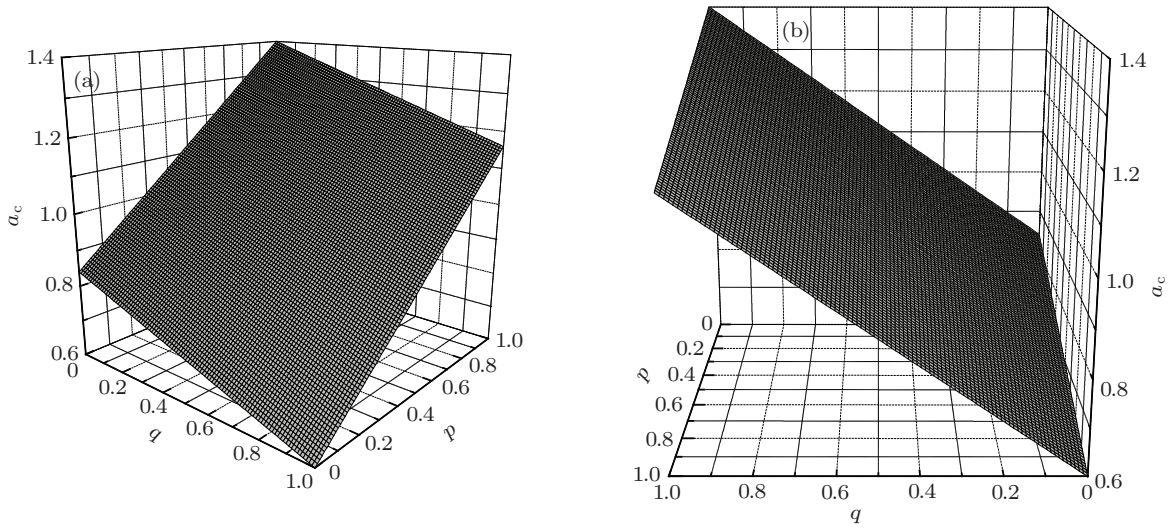


Fig. 6. Plots of the critical sensitivity a_c against the parameters q and p. (a) $c = 0.3$; (b) $c = 0.7$.

Figure 7 presents the plot of the critical sensitivity a_c against the value of fraction c with different values of q and p. When $q = 0.4$, $p = 0.2$ or $q = 0.4$, $p = 0.4$, the critical sensitivity a_c firstly increases and then decreases with increasing c. When $q = 0.4$, $p = 0.9$ or $q = p = 0.7$ or $q = 0.7$, $p = 0.9$, the critical sensitivity a_c decreases at the beginning and then increases with increasing c. When $q = 0.7$, $p = 0.2$, the criti-

cal sensitivity a_c decreases with increasing value of c. However, there is a common focal point at $c = 0.5$.

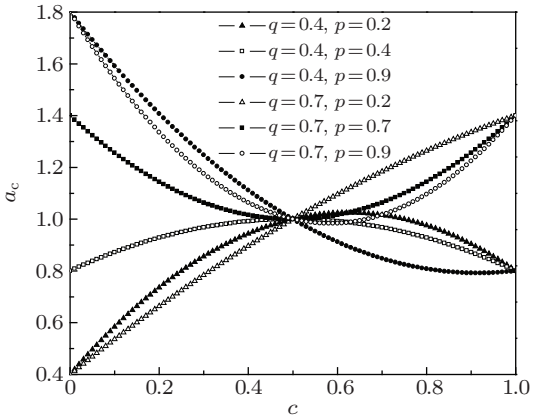


Fig. 7. Plot of the critical sensitivity a_c against the value of fraction c with different values of q and p.

6. Conclusion

We have proposed a new two-dimensional lattice hydrodynamic model with the turning capability of cars. We have investigated the jamming transition between the freely moving phase and the jammed phase both numerically and analytically. Based on this model, the stability condition and the mKdV equation describing the density wave of traffic congestion are obtained by using the linear stability theory and the nonlinear analysis method, respectively. There exist kink–antikink density waves in dense traffic. The numerical simulation is performed. It can also be found that the critical point of a_c increases with the increase of the fraction p of the northbound cars which continue to move along the positive y direction for $c = 0.3$, but the critical point of a_c decreases with the increase of the fraction p of the northbound cars for $c = 0.7$. The results indicate that the cars moving along only one direction (east or north) are most stable.

References

[1] Chowdhury D, Santen L and Schadschneider A 2000 *Phys. Rep.* **329** 199
[2] Helbing D 2001 *Rev. Mod. Phys.* **73** 1067
[3] Nagatani T 2002 *Rep. Prog. Phys.* **65** 1331
[4] Kerner B S and Konhäuser P 1993 *Phys. Rev.* E **48** 2335
[5] Kurtze D A and Hong D C 1995 *Phys. Rev.* E **52** 218
[6] Komatsu T and Sasa S 1995 *Phys. Rev.* E **52** 5574
[7] Muramatsu M and Nagatani T 1999 *Phys. Rev.* E **60** 180
[8] Nagatani T 1998 *Physica* A **261** 599
[9] Nagatani T 1999 *Physica* A **264** 581
[10] Nagatani T 1999 *Phys. Rev.* E **59** 4857
[11] Nagatani T 1999 *Physica* A **265** 297
[12] Nagatani T 1999 *Physica* A **272** 592
[13] Xue Y 2004 *Acta Phys. Sin.* **53** 25 (in Chinese)
[14] Ge H X, Dai S Q, Xue Y and Dong L Y 2005 *Phys. Rev.* E **71** 066119
[15] Ge H X and Cheng R J 2008 *Physica* A **387** 6952
[16] Zhu H B 2009 *Chin. Phys.* B **18** 1322
[17] Tang T Q, Huang H J and Xue Y 2006 *Acta Phys. Sin.* **55** 4026 (in Chinese)
[18] Peng G H 2010 *Acta Phys. Sin.* **59** 108 (in Chinese)
[19] Sun D H, Tian C and Liu W N 2010 *Chin. Phys.* B **19** 080514
[20] Peng G H, Cai X H, Liu C Q and Cao B F 2011 *Phys. Lett.* A **375** 2153
[21] Sun D H and Tian C 2011 *Acta Phys. Sin.* **60** 068901 (in Chinese)
[22] Tian J F, Jia B, Li X G and Gao Z Y 2010 *Chin. Phys.* B **19** 040303
[23] Tian H H, He H D, Wei Y Y, Xue Y and Lu W Z 2009 *Physica* A **388** 2895
[24] Xue Y, Tian H H, He H D, Lu W Z and Wei Y F 2009 *Eur. Phys. J.* B **69** 289
[25] Wen J, Tian H H and Xue Y 2010 *Acta Phys. Sin.* **59** 3817 (in Chinese)
[26] Cuesta J A, Martines F C, Molera J M and Sanchez A 1993 *Phys. Rev.* E **48** R4175
[27] Nagatani T 1994 *J. Phys. Soc. Jpn.* **63** 1228
[28] Nagatani T 1995 *J. Phys. Soc. Jpn.* **64** 1421